

Supporting Information

Thiadiazole Dioxide-Fused Picene: Acceptor Ability, Anion Radical Formation, and n-Type Charge Transport Characteristics

Yongfa Xie,^a Michio M. Matsushita^{*a} and Kunio Awaga^{*a,b}

^a Department of Chemistry & Research Center for Materials Science, Nagoya University, Furo-cho, Chikusa-ku, Nagoya 464-8602, Japan. E-mail: mmmatsushita@nagoya-u.jp, Awaga@mbox.chem.nagoya-u.ac.jp

^b CREST, JST, Furo-cho, Chikusa-ku, Nagoya 464-8602, Japan.

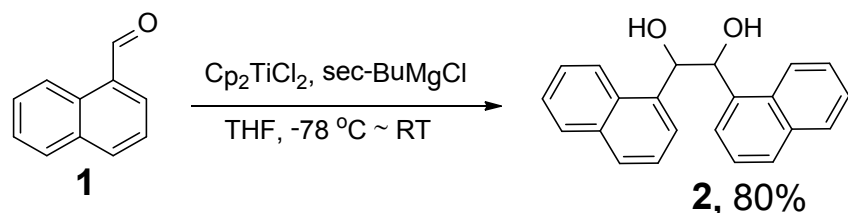
Contents

1. Experimental and calculation details	S2
2. Cyclic voltammogram and UV-vis characterization.....	S6
3. Calculation data of the anion radical species of PTDAO₂	S9
4. Crystal data and thin-film characterization.....	S11
5. NMR spectra of the compounds.....	S17

1. General Procedures

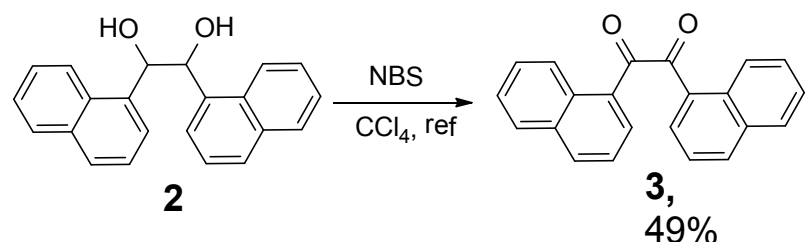
All chemicals and solvents purchased were used without further purification unless otherwise stated. NMR spectra were measured using 400 MHz or 600 MHz JEOL WinAlpha A-600 using TMS as internal reference. Low resolution and high resolution EI-MS spectra were measured using JOEL JMS-T100GCV with perfluorokerosene (PFK) as matrix. Cyclic voltammetry (CV) was carried out using HOKUTO DENKO HZ-5000 under nitrogen gas. UV-vis spectra were measured by JASCO V-570. Electron paramagnetic resonance (EPR) was measured by JOEL JES-FA 200 ESR spectrometer.

Syntheses and characterization of compounds



1,2-di(naphthalen-1-yl)ethane-1,2-diol (2).¹

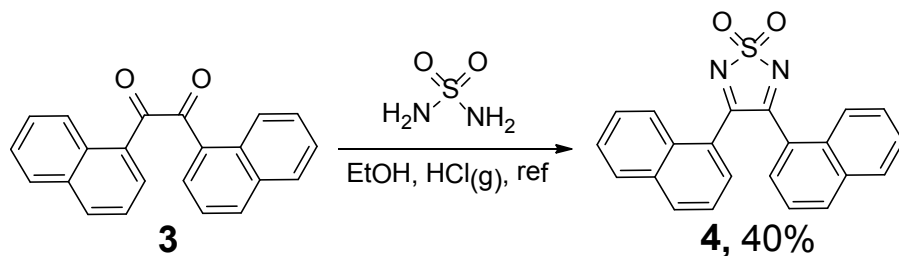
Sec-butylmagnesium chloride (sec-BuMgCl) (100 mL, 200 mmol, 2.0 M in ethyl ether) was added to a mixture of bis(cyclopentadienyl)titanium(IV) dichloride (Cp_2TiCl_2) (49.8 g, 200 mmol) in anhydrous tetrahydrofuran (180 mL) at -78 °C under N_2 gas. The mixture was stirred at -78 °C for 2 hours and then the temperature was allowed to slowly rise to room temperature for 0.5 hour. The mixture became a green suspension. 1-naphthaldehyde (23.4 g, 150 mmol) was slowly added to the mixture at -78 °C under N_2 gas. The mixture was stirred for 3 hours. The obtained black mixture was quenched with water (20 mL), filtered, and washed by ethyl ether. The filtrate was extracted with dichloromethane (300 mL × 3) and the combined organic layers were dried over Na_2SO_4 . After removing the solvent, the residue was purified by chromatography, eluting with hexane/ethyl acetate (2 : 1, 1 : 1) to afford a light yellow solid 18.7 g (yield: 80%). ^1H NMR (CDCl_3 , 600 MHz): δ 7.87~7.85 (2H, d, J = 8.4 Hz), 7.75~7.73 (2H, d, J = 8.4 Hz), 7.71~7.70 (2H, d, J = 7.8 Hz), 7.68~7.67 (2H, d, J = 7.2 Hz), 7.40~7.39 (2H, t, J = 8.1 Hz), 7.37~7.34 (2H, t, J = 7.5 Hz), 7.29~7.26 (2H, t, J = 7.8 Hz), 5.78 (2H, s), 2.99 (2H, s); ^{13}C NMR (CDCl_3 , 150 MHz): δ 136.23, 133.83, 131.04, 128.83, 128.76, 125.92, 125.50, 125.27, 124.99, 123.14, 74.58.



1,2-di(naphthalen-1-yl)ethane-1,2-dione (3).²

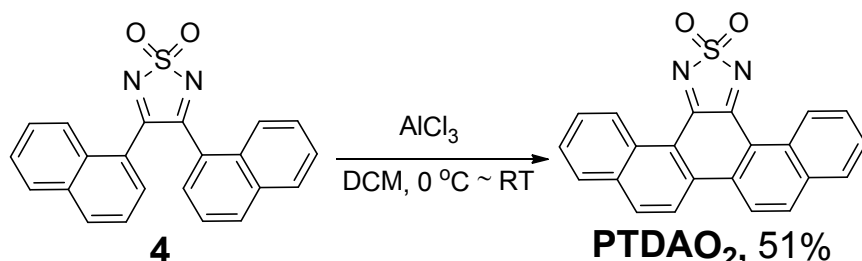
Compound 2 (9.6 g, 30.6 mmol) and N-Bromosuccinimide (13.6 g, 76.0 mmol) were added to CCl_4 (150 mL). The mixture was refluxed for 5 hours. The obtained red suspension was filtered, and washed by ethyl ether. The red filtrate was extracted with dichloromethane (500 mL × 2) and the combined organic layers were dried over Na_2SO_4 . After removing the solvent, the residue was purified by chromatography, eluting with hexane/dichloromethane (2 : 1, 1 : 1) to afford a yellow

solid 4.6 g (yield: 49%). ^1H NMR (CDCl_3 , 600 MHz): δ 9.36~9.35 (2H, d, J = 8.4 Hz), 8.14~8.12 (2H, d, J = 8.4 Hz), 8.04~8.02 (2H, d, J = 7.2 Hz), 7.97~7.95 (2H, d, J = 7.8 Hz), 7.77~7.75 (2H, t, J = 7.8 Hz), 7.66~7.63 (2H, t, J = 7.5 Hz), 7.51~7.48 (2H, t, J = 7.8 Hz); ^{13}C NMR (CDCl_3 , 150 MHz): δ 197.09, 135.92, 135.17, 134.31, 131.35, 129.55, 128.94, 127.24, 126.23, 126.21, 124.63.



3,4-di(naphthalen-1-yl)-1,2,5-thiadiazole 1,1-dioxide (4)

Compound **3** (3.0 g, 9.7 mmol) and sulfamide (4.5 g, 47.0 mmol) were added to anhydrous ethanol (50 mL). The mixture was refluxed for 8 hours, and HCl gas was introduced during the refluxing. The mixture was treated by water (50 mL), and extracted with dichloromethane (100 mL \times 2). The combined organic layers were dried over Na_2SO_4 . After removing the solvent, the residue was purified by chromatography, eluting with hexane/ethyl acetate (4 : 1, 3 : 1) to afford a yellow solid 1.03 g (yield: 40%). Crystals can be obtained by slow evaporation of the dichloromethane solution. Solubility in dichloromethane: > 10 mg/mL. IR ν_{max} = 3049 (w), 1529 (s), 1503 (s), 1343 (s), 1182 (s), 935 (m), 829 (m), 761 (m) cm^{-1} . High resolution EI-MS (M^+) for $\text{C}_{20}\text{H}_8\text{N}_2\text{S}_4$ found: 370.07756; calcd: 368.07760. ^1H NMR (CDCl_3 , 400 MHz): δ 8.30~8.28 (2H, m), 8.00~7.98 (2H, d, J = 8.3 Hz), 7.92~7.90 (2H, m), 7.60~7.56 (4H, m), 7.24~7.15 (4H, m); ^{13}C NMR (CDCl_3 , 100 MHz): δ 165.97, 134.13, 133.69, 130.93, 130.80, 129.05, 128.72, 127.43, 125.07, 124.89, 123.97.



Piceno[13,14-c][1,2,5]thiadiazole 14,14-dioxide (PTDAO₂)

Anhydrous aluminium chloride (0.74 g, 5.5 mmol) was added to a yellow solution of compound **4** (0.51 g, 1.4 mmol) in anhydrous dichloromethane (25 ml) at 0 °C under N_2 gas. The mixture was stirred at room temperature for 3 hours. The mixture was treated by ice-water (50 mL), and filtered. The filter cake was dried in a desiccator. 0.26 g light brown solid was obtained (yield: 51%). Crystals can be obtained by sublimation at 260 °C in the vacuum (~ 5.0 Pa) or by slow evaporation of the dichloromethane solution. Low solubility in dichloromethane: < 0.1 mg/mL. UV-vis absorption: $\lambda_{\text{max}} = 256\text{nm}$. IR ν_{max} = 3067 (w), 1516 (s), 1342 (s), 1163 (s), 816 (m), 745 (m) cm^{-1} . High resolution EI-MS (M^+) for $\text{C}_{20}\text{H}_8\text{N}_2\text{S}_4$ found: 368.0623; calcd: 368.0619. ^1H NMR (CDCl_3 , 600 MHz): δ 9.78~9.76 (2H, d, J = 7.2 Hz), 8.28~8.23 (4H, m), 7.91~7.89 (2H, d, J = 8.0 Hz), 7.82~7.80 (2H, t, J = 7.7 Hz), 7.66~7.64 (2H, t, J = 7.3 Hz); ^{13}C NMR can't be obtained due to the low solubility in common organic solvents.

Preparation of [TEA][PTDAO₂]

[TEA][PTDAO₂] was obtained by electrochemical reduction. Tetraethylammonium perchlorate (TEAP) (20.0 mg) was added to the both side tube of an H-shape cell as an electrolyte, and PTDAO₂ (6.0 mg) was added to one side of the H-shape tube. Then 1, 2-dimethylethanewas (DME) was added to the H-shape cell under N₂ gas. Current (0.5-0.9 μA) was applied to the solution by Pt electrode (PTDAO₂ is in the cathode). After 2 weeks, black needle-shaped crystals growed. The mixture was filtered and [TEA][PTDAO₂] was separated using microscope.

2. X-ray analysis.

Crystals were mounted on a loop using oil (CryoLoop, Immersion Oil, Type B; Hampton Research Corp.) and set on a Rigaku RA-Micro007 with a Saturn CCD detector using graphite-monochromated Mo Kα radiation ($\lambda = 0.710690 \text{ \AA}$) under a cold nitrogen steam. The frame data were integrated and corrected for absorption with the Rikagu/MSC CrystalClear package³. The structures were solved by direct methods⁴ and standard difference map techniques, and were refined with full-matrix least-square procedures on F^2 by a Rikagu/MSC CrystalStructure package. Anisotropic refinement was applied to all non-hydrogen atoms. All hydrogen atoms were placed at calculated positions and refined using a riding model.

3. Theoretical calculations.

The molecular orbital calculations based on density functional theory were carried out using the Gaussian09, revision C.01 program package. The molecular structures were optimized using HF and B3LYP⁵ methods with 6-31G(d) basis sets.

Intermolecular hopping carrier mobilities were calculated on the basis of Marcus theory.⁶ First, inter molecular electronic coupling matrix elements (V_{ab}) were calculated with equation 1 using intermolecular charge transfer integrals (H_{ab}), overlap integrals (S_{ab}), and the energies of the two molecular orbitals (H_{aa} and H_{bb}) calculated at PW91/TZ2P level using the ADF 2012 program package.

$$V_{ab} = \frac{H_{ab} - S_{ab}(H_{aa} - H_{bb}) / 2}{1 - S_{ab}^2} \quad (1)$$

Then the intermolecular charge transfer rate constants (k_{ET}) were evaluated from equation 2.

$$k_{ET} = \frac{V_{ab}^2}{h} \left(\frac{\pi}{\lambda k_B T} \right)^{1/2} \exp \left(-\frac{\lambda}{4k_B T} \right) \quad (2)$$

where, h , k_B , and T are Planck's constant, Boltzmann constant, and temperature, respectively. The reorganization energies upon intermolecular hole transfer (λ) were obtained from $\lambda = (E^{*-} - E^-) + (E^* - E)$. Where, E , E^- , E^* , and E^{*-} were the heat of formations for an optimized neutral molecule, optimized anion molecule, neutral state on anion structure, and anion state on neutral structure, respectively, calculated at B3LYP/6-31G(d) level. Intermolecular hopping mobilities (μ) were estimated from the following equation (3).

$$\mu_{hopping} = \frac{ed^2}{k_B T} k_{ET} \quad (3)$$

where, d is the intermolecular center-to-center distances of adjacent molecules.

4. Thin-film preparation and X-ray analysis.

Thin film of **PTDAO₂** was prepared by vapour deposition under a vacuum of 5×10^{-4} Pa. X-ray diffractions of thin films on bare Si substrates were obtained by Rikagu Smartlab X-ray diffractometer with a Cu K α source ($\lambda = 1.541 \text{ \AA}$) in air.

The interlayer spacing (d) determined from the first layer line of the thin-film XRD is 10.4 \AA which is close to the length of both b and c axes in the β phase crystal, so it is difficult to assign the molecular orientation on the substrate: The first sharp peak of the thin-film XRD is assignable for both reflection planes (001) and (010) as shown Figure S9(a). The possible two kinds of molecular orientation on the substrate are illustrated in Figure S9(b).

5. Fabrication of the thin-film transistors.

Bottom-contact, bottom-gate devices: thin films were deposited on Pt electrode with a gap of 2 μm over a 2 \times 2mm area (corresponding to 2 μm gap and 1 m width) as source/drain electrodes patterned on n-doped silicon substrates covered with 300nm-thick SiO₂ layer.

Top-contact, bottom-gate devices: thin films were deposited on silicon substrates covered with 300nm-thick SiO₂ layer, then Al was deposited on the thin films with channels of 30 μm or 100 μm at a deposition rate of 0.5 ~ 1.5 $\text{\AA}/\text{s}$.

Prior to deposition, the substrates were cleaned by sonication in acetone and isopropyl alcohol followed by exposure to O₂ plasma. Films were deposited by vacuum sublimation (pressure $\sim 5 \times 10^{-4}$ Pa) at a deposition rate 0.2 ~ 0.6 $\text{\AA}/\text{s}$. Organic field-effect transistor measurements were carried out in a vacuum with a Keithley 2636A dual channel source meter. The field-effect mobility (μ_{FET}) was calculated in the linear region of transfer curves.

6. Magnetic measurements

Magnetic susceptibility measurements were carried out on polycrystalline samples on a MPMS-XL Quantum Design magnetometer. All of the measurements used a plastic straw as the sample holder. Measurements for [TEA][PTDAO₂] were performed under 0.5 T in the temperature range of 2–300 K. The temperature dependences of the paramagnetic susceptibilities (χ_p) of the anion radical salts were calculated with paramagnetic susceptibilities obtained as fitting parameters.

$$\chi = \frac{N_A g^2 \mu_B^2}{k_B(T-\theta)} \frac{3 \exp(-2J/k_B T)}{1 + 3 \exp(-2J/k_B T)} \quad (4)$$

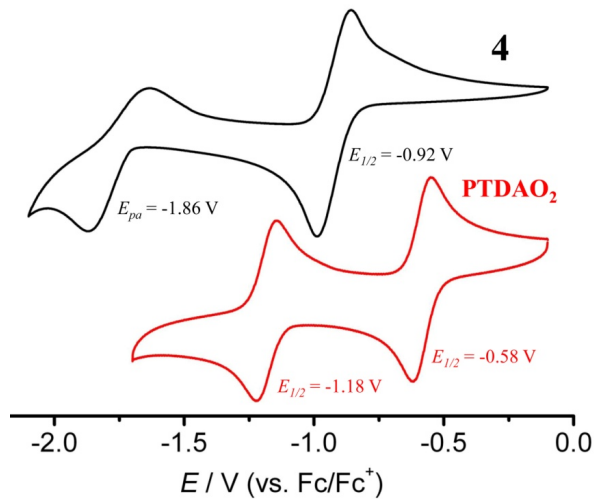


Figure S1. Cyclic voltammograms (scan rate 200 mV S⁻¹) of the precursor **4** and PTDAO₂ record in DCM solution containing *n*-Bu₄NClO₄ (0.1 M) as an electrolyte. Pt electrode was used as working electrode and counter electrode. Potentials referenced to Fc/Fc⁺.

Table S1. Electrochemical properties and theoretical energy levels

	4	PTDAO ₂	Picene ^f
$E_{1/2}^{\text{exp}} \text{ (V)}^a$	-0.92	-0.58	-2.76
$E_{1/2}^{\text{exp}} \text{ (V)}^a$	-1.86	-1.18	-3.16
$E_{\text{LUMO}}^{\text{exp}} \text{ (eV)}^b$	-3.88	-4.22	-2.04
$E_{\text{LUMO}}^{\text{calcd}} \text{ (eV)}^c$	---	-3.54	-1.27

^a From Cyclic voltammetry. ^b Estimated from the CV measurement according to the empirical formula $E_{\text{HOMO}} = -4.8 - E_{1/2}$ (vs. Fc/Fc⁺); $E_{1/2} = (E_{\text{pa}} - E_{\text{pc}})/2$ from reference 7a. ^c B3LYP/6-31G(d). ^f $E_{1/2}$ (Picene) = $E_{1/2}$ (ref. 7b) - $E_{1/2}$ (Ferrocene). $E_{1/2}$ (Ferrocene) = 0.55 V was determined in the same condition as reference 7b.

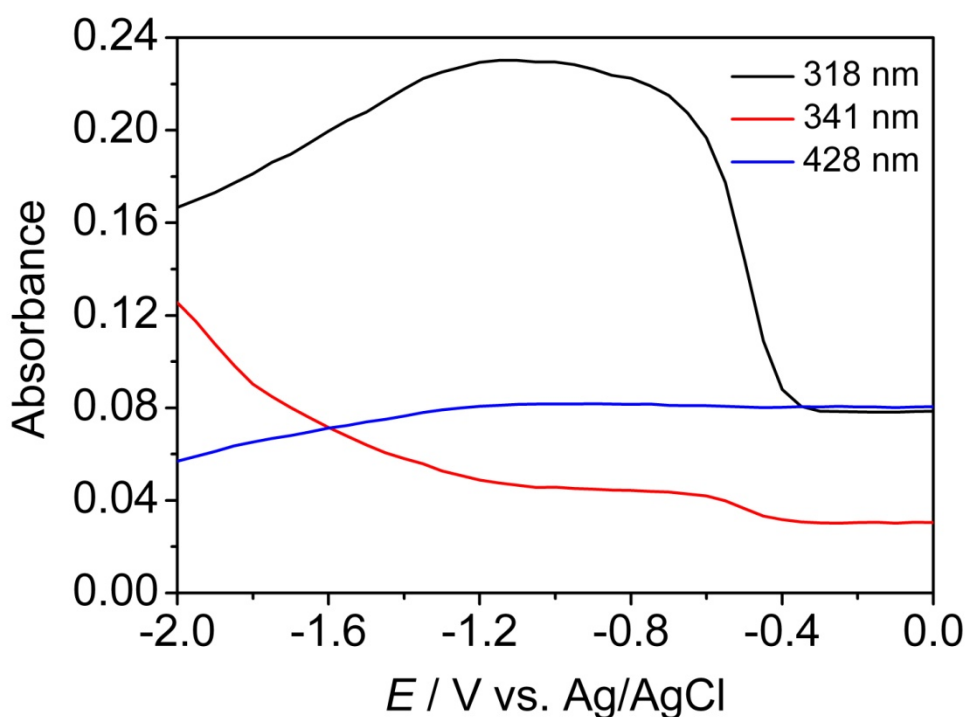


Figure S2. Potential dependence of the absorbance at selected wavelengths

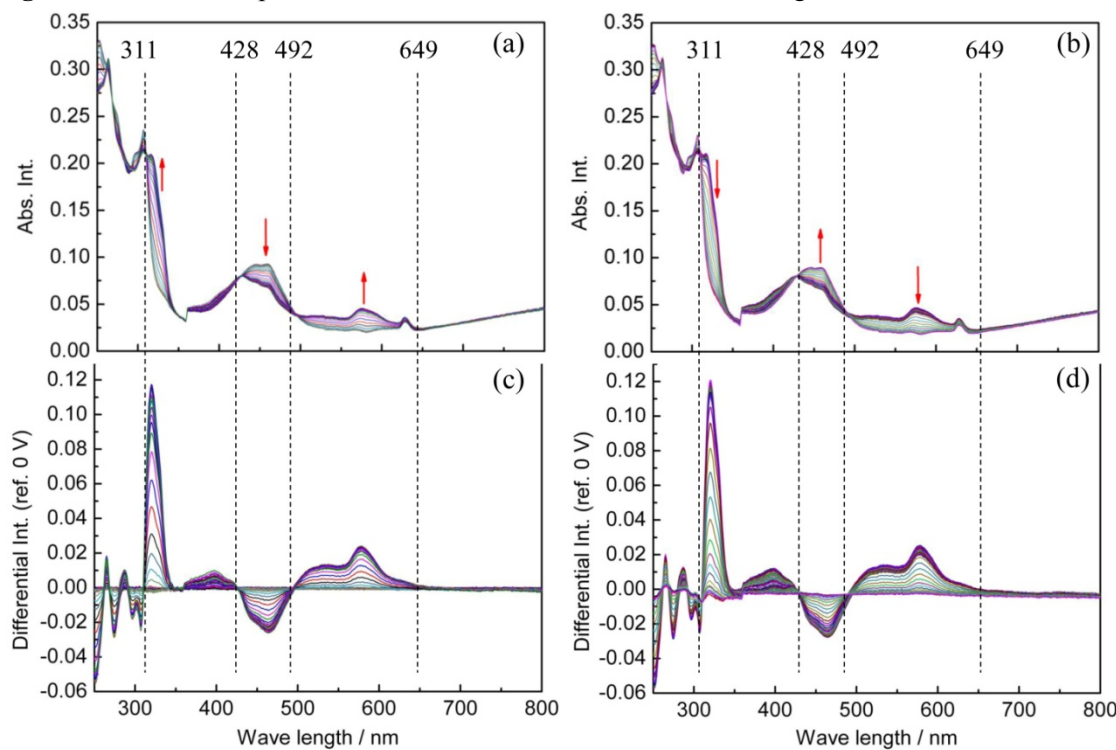


Figure S3. UV-Vis absorption spectra of **PTDAO₂** upon electro-reduction in 0.1 M *n*-Bu₄NClO₄ dichloromethane solution (scan rate: 0.1 mV s⁻¹; ref.: Ag/AgCl): (a) 0 V ~ -1 V, (b) -1 V ~ 0 V, (c) differential spectra from 0 V ~ -1 V, (d) differential spectra from -1 V ~ 0 V vs. Ag/AgCl.

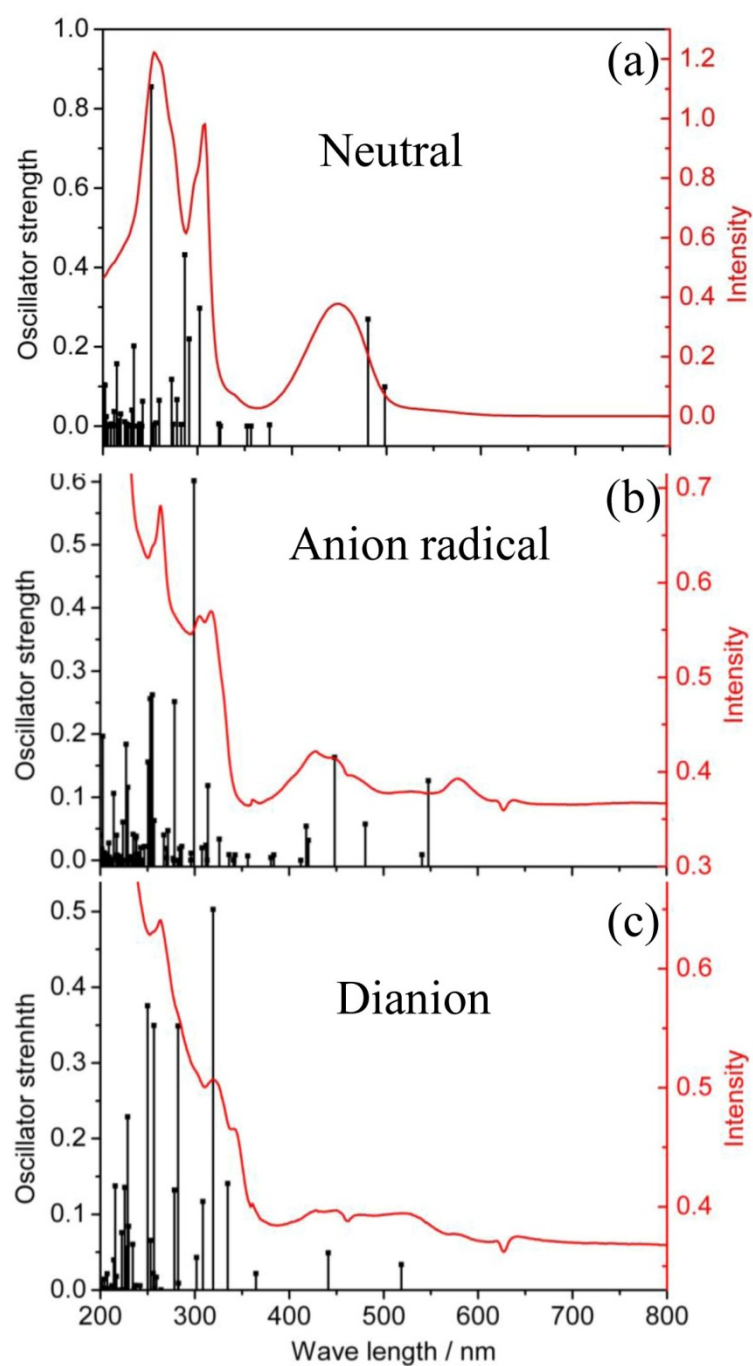


Figure S4. UV-vis absorption of PTDAO_2 (in CHCl_3) and theoretical calculation (B3LYP/6-31G(d)) (a), UV-vis absorption of anion radical of PTDAO_2 (in Dichloromethane) and theoretical calculation (UV-vis absorption spectrum is the in situ measurement with scanning voltage at -1.00 V. Theoretical data is calculated at UBLYP/6-31G(d)) (b), UV-vis absorption of dianion radical of PTDAO_2 (in Dichloromethane) and theoretical calculation. (UV-vis absorption spectrum is the situ measurement with scanning voltage at -2.00 V. Theoretical data is calculated at UBLYP/6-31G(d)) (c).

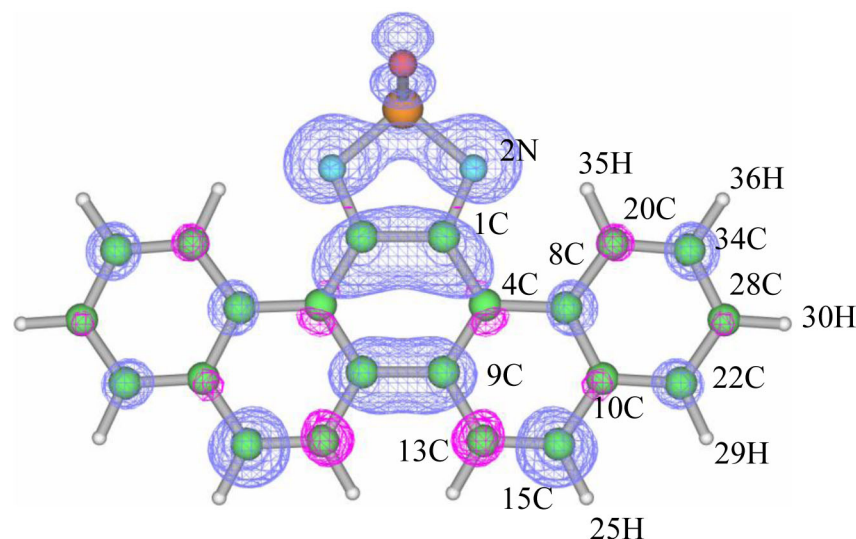


Figure S5. Calculated spin densities of **PTDAO₂** molecule with number scheme

Table S2. Spin densities of **PTDAO₂** radical obtained from the hyperfine coupling constants (a) of the EPR spectrum and the theoretical calculation

a (hyperfine)		Experimental values ^a			Theoretical values ^b		
N	H	N	C	H	N	C	H
0.29	---	0.116	---	---	0.245(2N)	---	---
						0.044(1C)	-0.001(35H)
0.26			0.106	0.0051		0.023(4C)	-0.0014(36H)
0.055			0.022	0.0011		0.012(8C)	0.0001(30H)
0.025			0.01	0.0005		-0.008(20C)	-0.0013(29H)
0.023			0.01	0.0005		0.026(34C)	-0.0041(25H)
						-0.007(28C)	0.0014(23H)
						0.026(22C)	
						-0.014(10C)	
						0.085(15C)	
						-0.041(13C)	
						0.064(9C)	

^a Spin densities were calculated from the hyperfine coupling constants according to the McConnell equation $a = Q\rho$ (Q (N) = 2.5 mT, Q (C) = 2.5 mT and Q (H) = 50.8 mT). ^b Theoretical spin densities were calculated by DFT method (UB3LYP/6-31G (d)). The corresponding atoms' numbers are shown in Figure S5.

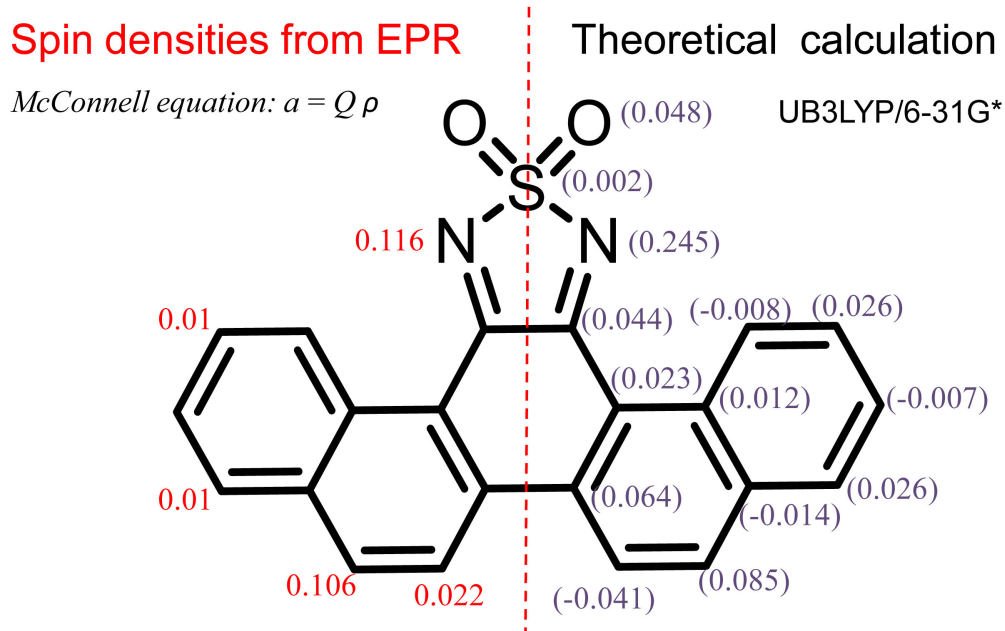


Figure S6. Comparison of experimental spin densities and theoretical spin densities of **PTDAO₂** radical

Table S3. Crystal data and intermolecular contacts

	4	PTDAO ₂ (α)	PTDAO ₂ (β)	[TEA][PTDAO ₂]
<i>Crystal system</i>	<i>monoclinic</i>	<i>orthorhombic</i>	<i>triclinic</i>	<i>triclinic</i>
Space group	<i>C2/c</i>	<i>Pbca</i>	<i>P\bar{I}</i>	<i>P\bar{I}</i>
<i>a</i> (Å)	19.249(5)	15.341(6)	7.175(4)	10.225(3)
<i>b</i> (Å)	11.102(3)	8.425(3)	10.612(5)	11.268(3)
<i>c</i> (Å)	8.547(2)	23.966(1)	10.682(5)	12.197(3)
α (deg)	---	---	97.969(9)	109.697(4)
β (deg)	106.665(4)	---	92.937(8)	105.9272(2)
γ (deg)	---	---	97.683(9)	92.225 (3)
$R(f > 2\sigma)$,	0.0349,	0.1097,	0.0535,	0.0414,
R_{w^2} (<i>all</i>)	0.0893	0.2642	0.1515	0.1106
$\delta(\text{\AA})^a$	---	---	3.412	---

^a π - π distance along the stacks.

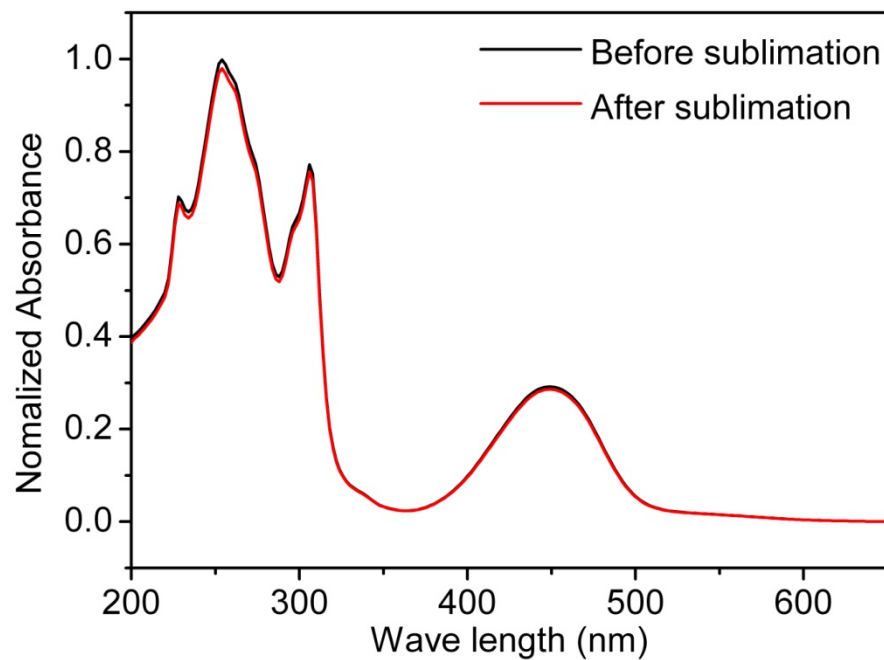


Figure S7. UV-vis absorption spectra of **PTDAO₂** before and after sublimation in dichloromethane solution

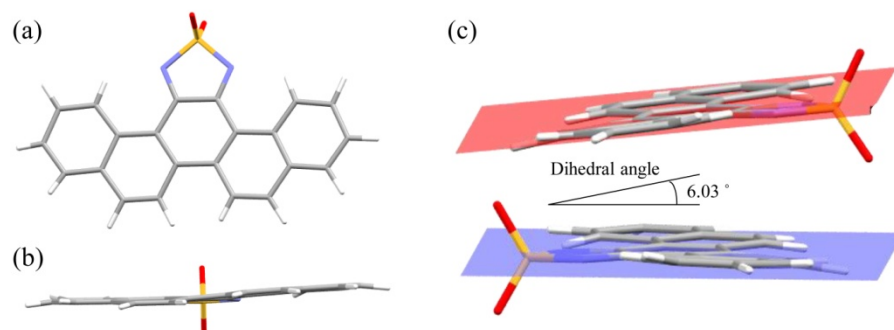


Figure S8. Crystal structure of **PTDAO₂** crystal obtained by sublimation. Top view (a) and side view (b). Intermolecular dihedral angle (c).

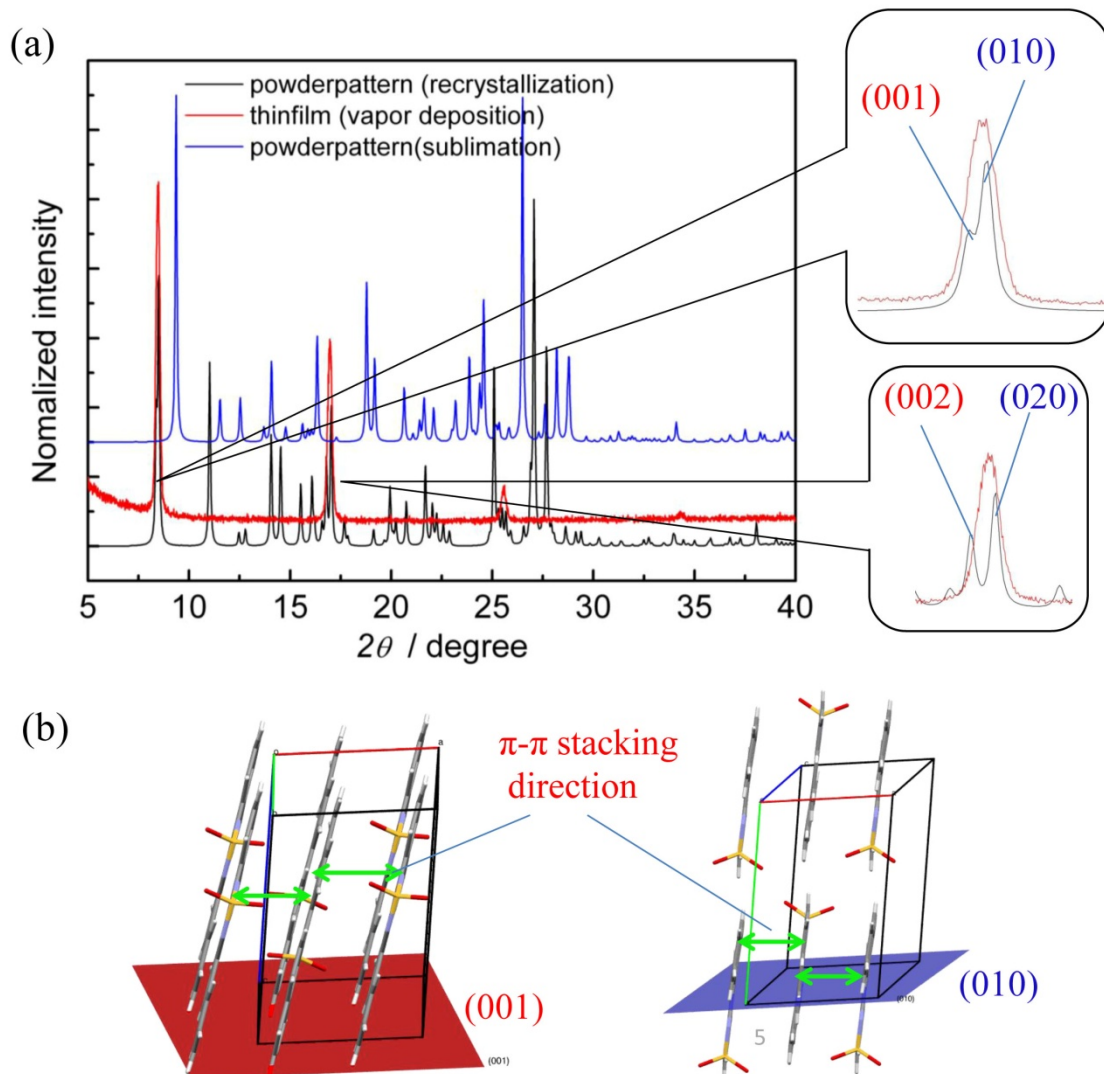


Figure S9. (a) Powder-pattern simulation of PTDAO_2 crystal recrystallized from DCM solution in black line; Out-of-plane XRD pattern of PTDAO_2 thin film (100nm) in red line; Powder-pattern simulation of PTDAO_2 crystal obtained by sublimation in blue line. Comparation of the thin-film XRD pattern and powder pattern is indicated by the enlarged figures. The crystal phase of the thin film of PTDAO_2 prepared by vapor deposition was assigned to the β -phase crystal which appears upon recrystallization from solution. (b) Molecular orientation on (001) and (010) planes.

Table S4. Electron mobilities (μ_e), current on/off ratios (I_{on}/I_{off}), and threshold voltage (V_T) for OFET devices based on **PTDAO₂**

Bottom contact, bottom gate, Pt as electrode, 60nm thin film					
Channel W/L	1m/2μm	0.4m/5μm	0.2m/10μm	0.1m/20μm	0.04m/50μm
$\mu_e / \text{cm}^2 \text{v}^{-1} \text{s}^{-1}$	1.0×10^{-4}	0.7×10^{-4}	1.2×10^{-4}	1.5×10^{-4}	0.3×10^{-4}
V_T / V	34	29	27	28	39
I_{on}/I_{off}	10^5	10^4	10^6	10^6	10^3
Bottom contact, bottom gate, Pt as electrode, 60nm thin film, channel W/L = 0.4m/2μm					
Surface treatment	HMDS			OTS	
$\mu_e / \text{cm}^2 \text{v}^{-1} \text{s}^{-1}$	0.7×10^{-4}			2.0×10^{-6}	
V_T / V	30			25	
I_{on}/I_{off}	10^3			10	
Bottom contact, bottom gate, Pt as electrode, 60nm thin film, channel W/L = 1m/2μm					
$T^a / \text{°C}$	r.t.	100	140	180	220
$\mu_e / \text{cm}^2 \text{v}^{-1} \text{s}^{-1}$	1.0×10^{-4}	1.4×10^{-4}	1.8×10^{-4}	1.6×10^{-4}	1.2×10^{-4}
Top contact, bottom gate, 100 nm thin film, Al as electrode					
Channel W/L	5cm/100μm			0.75cm/30μm	
$\mu_e / \text{cm}^2 \text{v}^{-1} \text{s}^{-1}$	0.3×10^{-4}			1.0×10^{-4}	
V_T / V	36			31	
I_{on}/I_{off}	10^6			10^4	

^a Annealing temperature of the OFET devices. Substrates were annealed for 30 min at each temperature under N₂ gas.

The charge mobility of OFET device of **PTDAO₂** was not sensitive for the film preparation method as described above. This could be explained as follows; as described at the thin-film X-ray diffraction section, the vapor-deposited thin film was assigned as the β -phase crystal, and the $\pi-\pi$ stacking direction (α -axis) is parallel to the substrate plane. This situation is favorable for the charge transportation. However, the other two axes (β - and γ -axes) in the β -phase crystal have very close periodicity, and it could not be distinguished in the thin film X-ray measurements. This result suggests that the close cell parameter cause the heavily disorder of the crystal direction at the substrate surface in the thin film and it increases the density of charge traps. The surface treatment by HMDS (hexamethyldisilazane) and OTS (octyltrichlorosilane) of the FET deviced did not improve the electron mobilities.

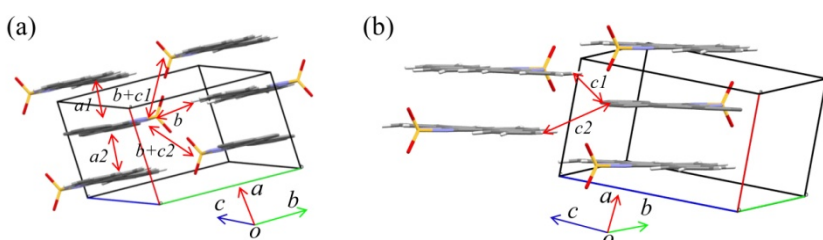


Figure S10. Effective intermolecular contacts in PTDAO_2 crystal along each axis

Table S5. Theoretical estimated intermolecular transfer intergrals (Hab), overlap intergrals (Sab), center-to-center distances (d), orbital interaction energy (V), reorganization energy (λ) and hopping mobilities for each molecular contact.

Contact ^a	Hab^b /meV	Sab^b /meV	d /Å	V /meV	λ^c /m eV	$\frac{\mu_{\text{hopping}}}{\text{cm}^2 \text{ V}^{-1} \text{ S}^{-1}}$
a_1	-150.6	15.8	4.120	-82.3	348.6	6.9×10^{-2}
a_2	-140.1	14.7	4.118	-76.8	348.6	6.0×10^{-2}
b	-14.4	1.7	10.235	7.4	348.6	3.4×10^{-3}
c_1	-3.5	0.4	10.682	-2.0	348.6	2.7×10^{-4}
c_2	2.0	-0.1	10.270	1.7	348.6	1.9×10^{-4}
$b+c_1$	-2.6	0.3	14.863	-1.2	348.6	1.8×10^{-4}
$b+c_2$	1.7	-0.2	13.975	0.9	348.6	9.1×10^{-5}
Pentacene^d	-165.6	---	---	---	94	$0.34 \sim 2.36$

^a Corresponding molecular contacts are indicated in Figure S10. ^b Calculated in PW91/TZ2P

level. ^c Calculated in B3LYP/6-31G(d) level. ^d Reference⁸

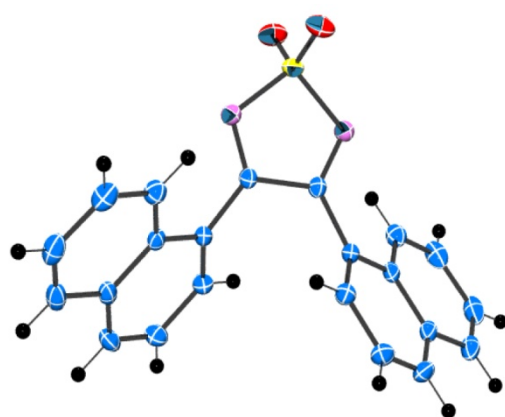


Figure S11. Crystal structure of compound 4 (Precursor of PTDAO_2)

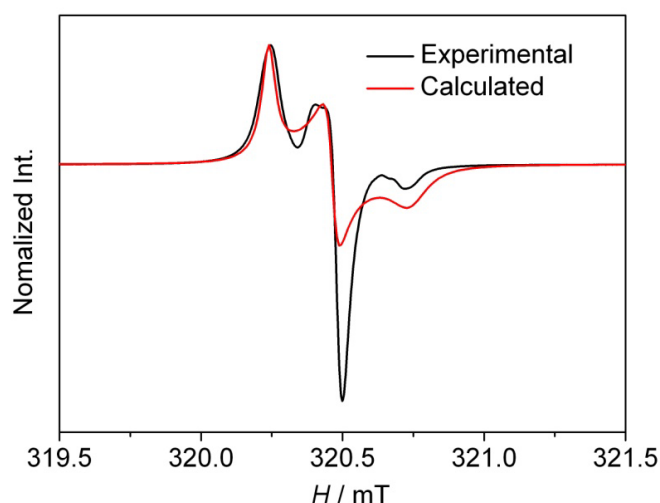


Figure S12. EPR spectrum of powdered crystals of $[\text{TEA}][\text{PTDAO}_2]$. Black line is experimental data measured at room temperature. Red line is theoretical calculation with anisotropic $g_x = 2.0066$, $g_y = 2.0052$, $g_z = 2.0035$.

References:

- (1) Y. Handa and J. Inanaga, *Tetrahedron Lett.*, 1987, 28, 5717-5718.
- (2) J. M. Khurana and B. M. Kandpal, *Tetrahedron Lett.*, 2003, 44, 4909-4912.
- (3) R. C. CrystalClear, 1999;; M. s. C. CrystalClear Software User's Guide, 2000; and J. W. Pflugrath, *Acta Crystallogr., Sect. D*, 1999, 55, 1718-1725.
- (4) G. M. Sheldrick, *SHELX97*, 1997.
- (5) P. J. Stephens, F. J. Devlin, C. F. Chabalowski and M. J. Frisch, *J. Phys. Chem.*, 1994, 98, 11623-11627.
- (6) (a) M. D. Newton, *Chem Rev*, 1991, 91, 767-792; (b) K. Senthilkumar, F. C. Grozema, F. M. Bickelhaupt and L. D. A. Siebbeles, *J. Chem. Phys.*, 2003, 119, 9809-9817; (c) K. Senthilkumar, F. C. Grozema, C. F. Guerra, F. M. Bickelhaupt, F. D. Lewis, Y. A. Berlin, M. A. Ratner and L. D. A. Siebbeles, *J. Am. Chem. Soc.*, 2005, 127, 14894-14903.
- (7) (a) A. Dadvand, F. Cicoira, K. Y. Chernichenko, E. S. Balenkova, R. M. Osuna, F. Rosei, V. G. Nenajdenko and D. F. Perepichka, *Chem. Commun.*, 2008, 5354-5356; (b) T. Saji and S. Aoyagi, *J. Electroanal. Chem.*, 1979, 98, 163-166.
- (8) S. Chai, S. H. Wen, J. D. Huang and K. L. Han, *J. Comput. Chem.*, 2011, 32, 3218-3225.

